

Trinucleon magnetic moments: 34-channel results

J. L. Friar and B. F. Gibson

Theoretical Division, Los Alamos National Laboratory, Los Alamos, New Mexico 87545

G. L. Payne

Department of Physics and Astronomy, University of Iowa, Iowa City, Iowa 52242

E. L. Tomusiak and M. Kimura*

Saskatchewan Accelerator Laboratory and Department of Physics, University of Saskatchewan, Saskatoon, Saskatchewan, Canada S7N 0W0

(Received 21 December 1987)

Impulse approximation and isovector pion-exchange current contributions to the trinucleon magnetic moments are calculated using wave functions generated from solutions of the configuration-space form of the Faddeev equations for the Reid soft core, Argonne V_{14} , and super-soft-core C nucleon-nucleon force models and the Tucson-Melbourne or Brazilian three-nucleon force models. Numerical results for solutions with two-body partial waves having $j \leq 4$ (up to 34 channels) are reported. Agreement between theory and experiment appears reasonable for these nonrelativistic Hamiltonians which are restricted to one-pion exchange currents.

I. INTRODUCTION

A variety of calculational techniques have been shown to yield reliable results for the solution of the Faddeev decomposition of the Schrödinger equation that describes the trinucleon ground state.¹ Using the same two-body interaction Hamiltonian, different authors have obtained remarkable agreement^{1,2} for the triton binding energy as well as for related physical observables such as the root-mean-square (rms) charge radii and wave function asymptotic normalization constants,^{3,4} which are determined primarily by the asymptotic (large radial distance) part of the wave function. However, such widespread agreement has not been seen in the case of the trinucleon magnetic moments. This may be partially attributed to detailed differences in the calculations of meson-exchange-current contributions to the magnetic moment operators. The status of magnetic moment calculations employing only nucleon-nucleon (two-body) forces in the Hamiltonian and truncating the three-body model space to five channels (two-body interactions in only the 1S_0 and 3S_1 - 3D_1 partial waves) has been summarized by Tomusiak *et al.*⁵

The rapid convergence in the calculation of trinucleon bound-state observables as a function of the number of two-body potential partial waves included in the Hamiltonian was demonstrated by Chen *et al.*¹ for a number of contemporary nucleon-nucleon potential models. However, the inclusion of a three-nucleon force in the Hamiltonian (in order to remove the discrepancy between theoretical and experimental values of the triton binding energy occurring in these two-body force model calculations) requires that many more three-body channels be incorporated in the calculation in order to achieve a converged result.^{6,7} For example, converged binding energies for model Hamiltonians that include either the Tucson-Melbourne (TM) or the Brazilian (BR) two-pion-exchange three-nucleon force requires at least 18 three-

body channels (all two-body partial waves with $j \leq 2$) to achieve a converged result and in several cases 34 three-body channels (all two-body partial waves with $j \leq 4$). Our purpose here is to report the results of new trinucleon magnetic moment calculations utilizing 34-channel wave functions from fully converged calculations with and without three-body forces in the model Hamiltonian.

The magnetic moment calculations described previously in Ref. 5 were based upon algebraic formulas which showed explicitly how the various wave function components contribute to the magnetic moment density. While such a procedure may help provide insight when only a few channels are involved, it is tedious and susceptible to error. Thus, we use a completely numerical approach here, where wave functions with as many as 34 channels are utilized. In comparing results with our previous calculations, minor errors in Ref. 5 were discovered and will be discussed at the appropriate junctures.

The material is organized as follows. We state the gen-

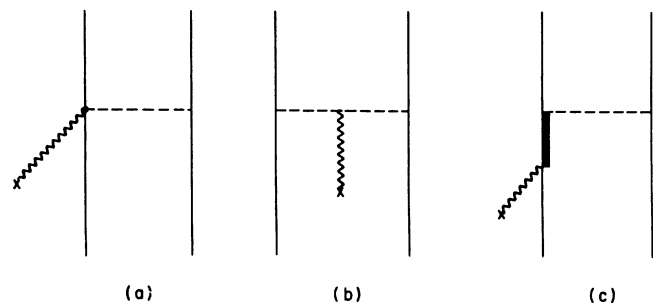


FIG. 1. Pion-exchange-current contributions: (a) seagull or pair diagram, (b) pion (true exchange) current diagram, and (c) Δ -isobar diagram.

TABLE I. Impulse approximation isoscalar and isovector magnetic moments.

Number of channels	RSC	RSC+TM	RSC+BR	AV14	AV14+TM	AV14+BR
	μ_s	μ_s	μ_s	μ_s	μ_s	μ_s
5	0.4044	0.4042	0.4019	0.4062	0.4058	0.4033
9	0.4041	0.4030	0.4000	0.4060	0.4049	0.4018
18	0.4041	0.4011	0.4003	0.4060	0.4031	0.4024
34	0.4038	0.4009	0.3998	0.4058	0.4031	0.4020
	μ_v	μ_v	μ_v	μ_v	μ_v	μ_v
5	-2.1492	-2.1548	-2.1447	-2.1659	-2.1717	-2.1600
9	-2.1496	-2.1555	-2.1440	-2.1660	-2.1719	-2.1587
18	-2.1550	-2.1549	-2.1500	-2.1724	-2.1712	-2.1660
34	-2.1549	-2.1537	-2.1489	-2.1722	-2.1706	-2.1647

eral formulas and values of the relevant parameters in Sec. II. The numerical methods are summarized in Sec. III. The numerical results for separate terms of the magnetic moment operator are presented in Sec. IV for 5-, 9-, 18-, and 34-channel wave functions. Finally, Sec. V provides a summary of the new results of this paper.

II. GENERAL FORMALISM

The nuclear current density at the point \mathbf{r} is denoted by $\mathbf{J}(\mathbf{r})$. The static magnetic moment operator is then given in terms of the current density by

$$\mu = \frac{1}{2} \int d\mathbf{r} \langle JM | [\mathbf{r} \times \mathbf{J}(\mathbf{r})]_z | JM \rangle, \quad (1)$$

where $M = J$. The current

$$\mathbf{J}(\mathbf{r}) = \mathbf{J}_{\text{imp}}(\mathbf{r}) + \mathbf{J}_{\text{ex}}(\mathbf{r}) + \Delta\mathbf{J}(\mathbf{r}) \quad (2)$$

comprises a one-body or impulse approximation contribution, a two-body or conventional pion-exchange current contribution, and an additional many-body contribution. The one-body current is composed of the standard convection and magnetization currents:

$$\begin{aligned} \mathbf{J}_{\text{imp}}(\mathbf{r}) = & \frac{1}{2M_p} \sum_i \left[\frac{1+\tau_3(i)}{2} \right] [\mathbf{p}_i \delta(\mathbf{r}-\mathbf{x}_i) + \delta(\mathbf{r}-\mathbf{x}_i) \mathbf{p}_i] \\ & + \nabla \times \sum_i \left[\frac{1+\tau_3(i)}{2} \mu_p \right. \\ & \left. + \frac{1-\tau_3(i)}{2} \mu_n \right] \boldsymbol{\sigma}(i) \delta(\mathbf{r}-\mathbf{x}_i). \quad (3) \end{aligned}$$

In Eq. (3) we use values of $\mu_p = 2.793\mu_N$ and $\mu_n = -1.913\mu_N$, where $\mu_N = e\hbar/2M_p c$ is the nuclear magneton. The exchange current term $\mathbf{J}_{\text{ex}}(\mathbf{r})$ is comprised of the usual ‘‘pair+pion+isobar’’ pieces detailed below. Any nucleon-nucleon interaction based upon the exchange of charged quanta will lead to two-body exchange current contributions to the electromagnetic operators describing the system. Similarly, when a two-pion-exchange three-nucleon force is included in the Hamiltonian, corresponding three-body exchange-current terms $[\Delta\mathbf{J}(\mathbf{r})]$ arise in the electromagnetic current. However, such three-nucleon currents should contribute in the same order as the relativistic corrections to the two-nucleon currents which we neglect. (We also omit effects from heavy meson exchange, which are estimated to be a

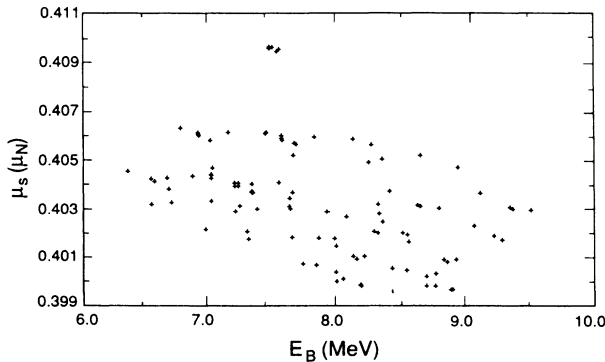


FIG. 2. Trinucleon isoscalar magnetic moment plotted vs the binding energy.

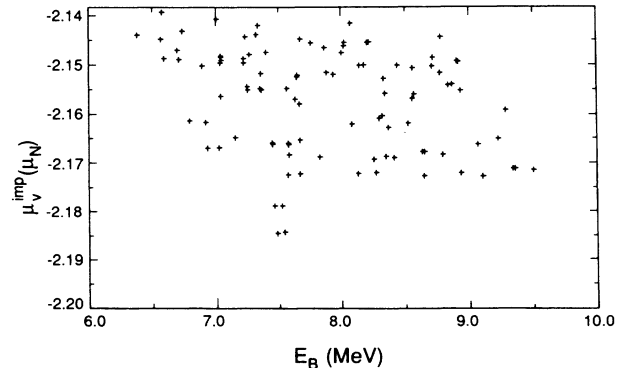


FIG. 3. Impulse approximation trinucleon isovector magnetic moment plotted vs the binding energy.

TABLE II. Pair diagram contributions to μ_v ($\Lambda = 5.8m_\pi$).

Number of channels	Potential					
	RSC	RSC+TM	RSC+BR	AV14	AV14+TM	AV14+BR
5	-0.2820	-0.2848	-0.2955	-0.2878	-0.2958	-0.3062
9	-0.2864	-0.3034	-0.3228	-0.2904	-0.3114	-0.3293
18	-0.2835	-0.3155	-0.3161	-0.2877	-0.3227	-0.3201
34	-0.2859	-0.3135	-0.3186	-0.2896	-0.3194	-0.3220

10% correction to the dominant one-pion-exchange term). Therefore, to be consistent we omit specific contributions to the magnetic moment operator from three-nucleon exchange currents at this time.

The terms which we retain in our calculation of the isovector pion-exchange-current contributions to the trinucleon magnetic moments are⁸

$$\mathbf{J}_{\text{ex}}(\mathbf{r}) = \mathbf{J}_{\text{pair}}(\mathbf{r}) + \mathbf{J}_\pi(\mathbf{r}) + \mathbf{J}_\Delta(\mathbf{r}). \quad (4)$$

(Isoscalar terms are corrections of relativistic order.⁹) The pair term results from the seagull diagram shown in Fig. 1(a). That current operator is

$$\mathbf{J}_{\text{pair}}(\mathbf{r}) = \frac{f^2}{m_\pi^2} \sum_{i \neq j} [\boldsymbol{\tau}(i) \times \boldsymbol{\tau}(j)]_3 \boldsymbol{\sigma}(i) \delta(\mathbf{r} - \mathbf{x}_i) \times [\boldsymbol{\sigma}(j) \cdot \nabla_r] h_0(|\mathbf{r} - \mathbf{x}_j|), \quad (5)$$

where the pion-nucleon form factor is assumed to have the monopole form

$$h_0(r) = \frac{1}{r} \left[e^{-m_\pi r} - e^{-\Lambda r} - \frac{\Lambda r}{2} \left[1 - \frac{m_\pi^2}{\Lambda^2} \right] e^{-\Lambda r} \right]. \quad (6)$$

Similarly, the pion current or true-exchange current operator depicted in Fig. 1(b) is given by

$$\mathbf{J}_\pi(\mathbf{r}) = \frac{-f^2}{8\pi m_\pi^2} \sum_{i \neq j} [\boldsymbol{\tau}(i) \times \boldsymbol{\tau}(j)]_3 [\boldsymbol{\sigma}(i) \cdot \nabla_r \tilde{h}_0(|\mathbf{r} - \mathbf{x}_i|)] \tilde{\nabla}_r \times [\boldsymbol{\sigma}(j) \cdot \nabla_r \tilde{h}_0(|\mathbf{r} - \mathbf{x}_j|)], \quad (7)$$

where

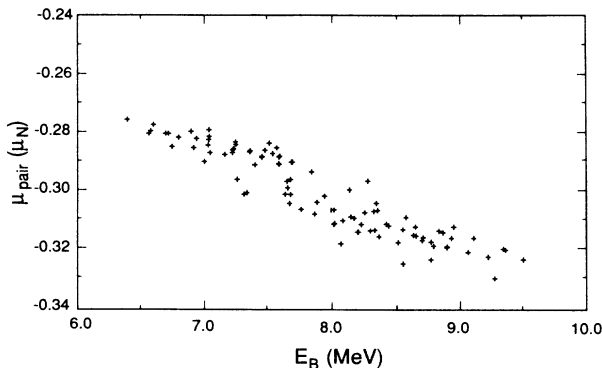


FIG. 4. Trinucleon pair current contribution to the isovector magnetic moment plotted vs the binding energy.

$$\tilde{h}_0(r) = \frac{1}{r} [e^{-m_\pi r} - e^{-\Lambda r}]. \quad (8)$$

We note here that the tilde symbol in $\tilde{h}_0(r)$ was inadvertently omitted in the corresponding Eq. (16) of Ref. 5. The Δ or isobar current shown in Fig. 1(c) is given by

$$\mathbf{J}_\Delta(\mathbf{r}) = \frac{8}{25} \frac{f^2}{m_\pi^2} \frac{\mu_p - \mu_n}{2M_p(M_\Delta - M_p)} \nabla_r \times \sum_{i \neq j} \delta(\mathbf{r} - \mathbf{x}_i) \{ [\boldsymbol{\sigma}(i) \times \nabla_r] [\boldsymbol{\tau}(i) \times \boldsymbol{\tau}(j)]_3 - 4\tau_3(j) \nabla_r \} \boldsymbol{\sigma}(j) \cdot \nabla_r h_0(|\mathbf{r} - \mathbf{x}_j|). \quad (9)$$

The uncertainty in this last term is the largest, due to various allowed prescriptions for choosing the $\gamma N \Delta$ coupling constant and for treating the Δ propagator.

We have used in these calculations a value of $f^2 = 0.078$. The mass values were $m_\pi = 140$ MeV, $M_p = 938.9$ MeV, and $M_\Delta = 1232$ MeV. For the monopole form factor cutoff, we use $\Lambda = 5.8m_\pi$, as current practice suggests.¹⁰ However, we will exhibit the dependence of the exchange current contribution to the magnetic moments upon the parameter Λ .

III. SUMMARY OF NUMERICAL METHODS

The magnetic moment is given in Eq. (1) in terms of the matrix element

$$\langle \Omega \rangle = \langle JM | [\mathbf{r} \times \mathbf{J}(\mathbf{r})]_z | JM \rangle. \quad (10)$$

Using the Wigner-Eckart theorem one can rewrite that matrix element in the form

$$\langle \Omega \rangle = (JM10 | JM) \langle J || [\mathbf{r} \times \mathbf{J}(\mathbf{r})] || J \rangle, \quad (11)$$

where we have used the conventions defined in Brink and Satchler.¹¹ For $J = M = \frac{1}{2}$, the Clebsch-Gordan coefficient has the value $1/\sqrt{3}$. The calculation reduces to the numerical evaluation of the reduced matrix element $\langle J || [\mathbf{r} \times \mathbf{J}(\mathbf{r})] || J \rangle$.

For three particles with coordinates \mathbf{r}_i in the center of mass we introduce the Jacobi variables

$$\mathbf{x}_i = \mathbf{r}_j - \mathbf{r}_k, \quad (12a)$$

and

$$\mathbf{y}_i = \frac{1}{2}(\mathbf{r}_j + \mathbf{r}_k) - \mathbf{r}_i, \quad (12b)$$

TABLE III. Pion current contributions to μ_v ($\Lambda = 5.8m_\pi$).

Number of channels	Potential					
	RSC	RSC+TM	RSC+BR	AV14	AV14+TM	AV14+BR
5	0.0851	0.0882	0.0906	0.0917	0.0988	0.1002
9	0.0873	0.0975	0.1041	0.0930	0.1073	0.1122
18	0.0857	0.1020	0.1033	0.0914	0.1113	0.1068
34	0.0868	0.1005	0.1015	0.0922	0.1091	0.1076

with i, j, k cyclic. Using these coordinates the operator in the reduced matrix element can be written in the form

$$\Omega = T_{KQ}[T_{k_1 q_1}(\mathbf{r}, \mathbf{x}_1, \mathbf{y}_1), T_{k_2 q_2}(\boldsymbol{\sigma}_1, \boldsymbol{\sigma}_2, \boldsymbol{\sigma}_3)] \times T_{kq}(\boldsymbol{\tau}_1, \boldsymbol{\tau}_2, \boldsymbol{\tau}_3) \quad (13)$$

for each of the various current operators, where the T_{kq} are tensor operators. Given the operators in Eq. (13) we have to evaluate the reduced matrix element

$$\langle J || [\mathbf{r} \times \mathbf{J}(\mathbf{r})] || J \rangle = \langle \Psi || \Omega || \Psi \rangle \quad (14)$$

using the total wave function generated by our configuration space Faddeev program. This wave function is given in terms of a bicubic spline expansion¹² and

the angular momentum-spin-isospin channel functions. Given the numerical solution to the Faddeev equations for the trinucleon system, it was shown in Ref. 13 that the total wave function could be written in the form

$$\Psi(\mathbf{x}_1, \mathbf{y}_1) = \sum_n \sum_L \sum_{M_L} (LM_L S_n M_S | JM) \Psi_{LM_L}^n(\mathbf{x}_1, \mathbf{y}_1) \phi_n, \quad (15)$$

where the ϕ_n are the spin-isospin functions defined by Gibson and Schiff¹⁴ with total spin S_n and total isospin T_n . Using this form of the wave function, the reduced matrix element in Eq. (14) can be written as

$$\langle \Psi || \Omega || \Psi \rangle = \sum_n \sum_{L, L'} [(2J+1)(2K+1)(2L'+1)(2S_{n'}+1)]^{1/2} \begin{Bmatrix} J & J & K \\ L' & L & k_1 \\ S_{n'} & S_n & k_2 \end{Bmatrix} \langle \Psi_{L'}^{n'} || T_{k_1} || \Psi_L^n \rangle \langle \phi_{n'} || T_{k_2} T_k || \phi_n \rangle. \quad (16)$$

The reduced matrix element of the spin-isospin operators may be evaluated analytically using standard Raçah algebra. The reduced matrix element of T_{k_1} must be evaluated numerically. To evaluate this integral we use the relationship

$$\langle \Psi_{L'}^{n'} || T_{k_1} || \Psi_L^n \rangle = \frac{1}{2L'+1} \sum_{M, M'} (LM k_1 q_1 | L' M') \times \langle \Psi_{L' M'}^{n'} | T_{k_1 q_1} | \Psi_{L M}^n \rangle. \quad (17)$$

The six-dimensional integral over \mathbf{x}_1 and \mathbf{y}_1 can be re-

duced to a three-dimensional integral by using the procedure originally suggested by Balian and Brezin.¹⁵ This procedure uses a convenient coordinate system to numerically evaluate the integral. Since the reduced matrix element is independent of the orientation of the coordinate axes, we can choose these axes so that the numerical calculations are simplified. Following Ref. 15 we choose the axes so that \mathbf{y}_1 is along the z axis and \mathbf{x}_1 is in the x - z plane. Now all of the vectors \mathbf{x}_i and \mathbf{y}_i will lie in the x - z plane. All of the current operators except for the pion current have a $\delta(\mathbf{r} - \mathbf{x}_i)$, and the vector \mathbf{r} will also be in the x - z plane. For these cases the integral is reduced to a three-dimensional integral over x_1, y_1 , and the angle between \mathbf{x}_1 and \mathbf{y}_1 . For the pion current operator, it was shown in Ref. 5 that the integral of the operator over \mathbf{r} could be expressed in terms of x_1, y_1 , and $\hat{\mathbf{x}}_1 \cdot \hat{\mathbf{y}}_1$. Using

TABLE IV. Isobar contributions to μ_v ($\Lambda = 5.8m_\pi$).

Number of channels	Potential					
	RSC	RSC+TM	RSC+BR	AV14	AV14+TM	AV14+BR
5	-0.0978	-0.1017	-0.1063	-0.0976	-0.1046	-0.1092
9	-0.0998	-0.1100	-0.1189	-0.0988	-0.1111	-0.1194
18	-0.0994	-0.1167	-0.1157	-0.0983	-0.1174	-0.1146
34	-0.1007	-0.1153	-0.1174	-0.0994	-0.1151	-0.1158

TABLE V. Isovector magnetic moments.

Number of channels	Potential					
	RSC	RSC+TM	RSC+BR	AV14	AV14+TM	AV14+BR
5	-2.4439	-2.4531	-2.4559	-2.4597	-2.4732	-2.4753
9	-2.4485	-2.4714	-2.4816	-2.4622	-2.4871	-2.4953
18	-2.4521	-2.4851	-2.4815	-2.4670	-2.5000	-2.4939
34	-2.4548	-2.4821	-2.4834	-2.4690	-2.4961	-2.4950

this expression the contribution of the pion current to the total magnetic moment can also be reduced to a three-dimensional integral. For a more detailed discussion of numerical calculations similar to those outlined here, the dissertation of Chen¹⁶ should be consulted.

IV. RESULTS

To nonrelativistic order (f^2/m_π^2), the isoscalar currents are given solely by the one-body terms.⁹ That is, the exchange terms contribute to the isoscalar currents only through relativistic terms which we have neglected. Thus, the nonrelativistic isoscalar magnetic moments are determined solely by the impulse approximation current of Eq. (3). As discussed in Ref. 5, an approximate formula is

$$\mu_s \simeq \frac{\mu_p + \mu_n}{2} [1 - 2P(D)] + \frac{1}{2}P(D) \quad (18)$$

$$\simeq 0.44 - 0.38P(D), \quad (19)$$

where $P(D)$ is the trinucleon wave function D -state probability.¹⁷ For contemporary nucleon-nucleon (NN) potentials which yield a value of $P(D)$ between 7% and 10%, one finds a value of μ_s between 0.41 and 0.40. The addition of a three-body force of the Tucson-Melbourne¹⁸ or Brazilian¹⁹ type to the nuclear Hamiltonian leads to an enhancement of $P(D)$ of about 1%, which reduces slightly the corresponding value of μ_s . This is illustrated by the results of our calculations for 5-, 9-, 18-, and 34-channel wave functions as summarized in Table I. In

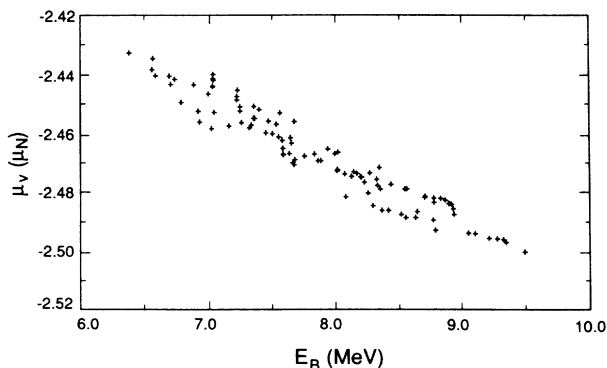


FIG. 5. Trinucleon isovector magnetic moment plotted vs the binding energy.

combination with the Reid-soft-core²⁰ (RSC) NN force model, both the TM and BR three-body force models lead to an isoscalar magnetic moment estimate of $\mu_s \simeq 0.40$. A similar conclusion holds for the Argonne V_{14} (AV14) (Ref. 21) NN potential model. Calculations have also been performed using various combinations of two-body forces [RSC, RSCC (including a Coulomb interaction between the two protons), AV14, and super soft core C (SSCC) (Ref. 22)] and three-body forces (TM and BR) and with varying numbers of channels. That “data set” provides a basis for an analysis of the dependence of the various components of the magnetic moments upon the binding energy. In Fig. 2 we present a scatter plot of the calculated isoscalar magnetic moments versus the model trinucleon binding energies. The calculated values of μ_s lie between 0.40 and 0.41. Little correlation with binding energy is exhibited, because Eqs. (18) and (19) demonstrate that μ_s depends principally upon the D state. Including three-body forces and varying the number of channels alters the relationship between $P(D)$ and the binding energy. Furthermore, the quoted experimental value of $\mu_s = 0.426$ clearly lies outside the range of theoretical values, indicating the need for a correction of order 5–6%.

With this understanding of the isoscalar approximation, we turn to the trinucleon isovector magnetic moments. As was discussed in Ref. 5, the impulse term contribution is given approximately by

$$\mu_v = -\frac{\mu_p - \mu_n}{2} [1 - \frac{4}{3}P(S') - \frac{2}{3}P(D)] + \frac{1}{6}P(D). \quad (20)$$

For typical model probabilities of $P(S') = 1\%$ and $P(D) = 10\%$, we obtain $\mu_v \simeq -2.15$. Indeed, as one can see from the values quoted in Table I and the larger data set plotted in Fig. 3, the impulse approximation to the isovector magnetic moment ranges in value from -2.14 to -2.18 . As was observed for μ_s , the impulse approximation for μ_v appears to have no strong correlation with the binding energy.

As noted previously, the first-order corrections (the two-body exchange currents) to the isovector impulse approximation are not of relativistic order. They yield, in fact, approximately a 20% enhancement of the magnitude. It was shown in Ref. 5 that the pair diagram [Fig. 1(a)] term provides the dominant exchange current contribution to μ_v . Unfortunately, there was a slight error in the values of μ_{pair} given in Ref. 5, which changes the total magnetic moment μ_v by 2–3% for $\Lambda = 5.8 m_\pi$.²³ Corrected values are given along with the new results in

TABLE VI. Variation of isovector magnetic moments with Λ for the 34-channel wave function, RSC model.

$\Lambda(m_\pi)$	μ_{pair}	μ_π	μ_Δ	μ_ν
2.0	-0.077	+0.0365	-0.010	-2.205
4.0	-0.228	+0.0811	-0.059	-2.361
5.8	-0.286	+0.0868	-0.101	-2.455
8.6	-0.318	+0.0830	-0.143	-2.533
17.2	-0.332	+0.0733	-0.180	-2.594

Table II and Fig. 4. The correlation with binding reflects the enhanced overlap as the wave function is pulled in. The pion current contributes to μ_ν at the 5% level. Specific contributions for the potential models listed above are detailed in Table III. As was the case for the pair current, including either the TM or BR three-body force in the Hamiltonian enhances the magnitude of μ_π by about 10% compared to the pure nucleon-nucleon force model results. Although the two-body force results presented here agree with those given in Ref. 5, we note that the statement there that the D - D matrix elements vanish identically is erroneous. The D - D matrix elements are tiny but are, in fact, nonzero. Our results for the isobar contribution to μ_ν are listed in Table IV. As described in Ref. 5, there is a large cancellation between μ_Δ and μ_π , which can be seen here by comparing Tables III and IV. Again, including a three-body force produces a 10% effect. The results for the 5-channel RSC and AV14 models differ from those in Ref. 5 by about 3% due to a phase error involving the P states in the μ_Δ calculation.²⁴

The total isovector magnetic moment (for $\Lambda=5.8m_\pi$) is the sum of the impulse approximation and the exchange current contributions contained in Tables I–IV. These are summed explicitly for the RSC and AV14 models in Table V. In Fig. 5 we plot μ_ν versus the trinucleon binding energy for all models studied. Again, the increase in μ_ν with increased binding reflects the enhancement of the overlap in μ_{pair} as the size of the system shrinks. Our model value for μ_ν ranges from -2.44 to -2.50. The experimental value of $\mu_\nu = -2.5532$ does not lie within this range. However, relativistic and heavy-meson exchange corrections of a few percent could easily account for the discrepancy.

More important than the small corrections omitted is the variation with the value of the cutoff Λ used in the

model calculations. This is illustrated in Table VI for the RSC potential model 34-channel wave function. (Results for the 5-channel wave function differ by only a few percent.) Clearly, this is the parameter to which the model calculation is most sensitive.

Using the currently favored¹⁰ value of $\Lambda=5.8m_\pi$, we summarize in Table VII our results for μ_s and μ_ν as well as $\mu(^3\text{He})$ and $\mu(^3\text{H})$ from the RSC and AV14 potential models with and without the TM and BR three-body forces. The discrepancy between our model results and experiment is clear. We reiterate that we have included no relativistic or heavy-meson corrections and that the model results are sensitive to the value of the cutoff Λ used in the exchange current operators. Furthermore, in keeping with our neglect of terms of relativistic order, we have neglected all three-body current contributions to the magnetic moments.

V. SUMMARY AND CONCLUSIONS

We have calculated the isoscalar and isovector magnetic moments of the trinucleons using model Hamiltonians based upon contemporary nucleon-nucleon potentials and those also including two-pion-exchange three-nucleon forces of the Tucson-Melbourne and Brazilian type. The difference in model results for μ_s and μ_ν between the 5-channel and full 34-channel wave functions, when only two-body forces are included, is less than 1%. The introduction of a three-body force improves the agreement between the calculated value of μ_ν and the experimental value by enhancing the meson-exchange current contribution. (The value of μ_s is modified only slightly by the introduction of a three-body force.) Using the preferred value of the cutoff ($\Lambda=5.8m_\pi$), one sees a difference between experimental and theoretical values for μ_ν of about 0.06 and for μ_s of about 0.03. The dependence upon the model binding energy is very weak: a 2% variation in the magnetic moments for a 15% change in the binding energy. Conversely, the calculations are clearly sensitive to the value of the cutoff Λ used. Increasing it by a small percentage would produce exact agreement for μ_ν . However, all relativistic corrections have been ignored in these calculations, as well as heavier meson exchanges. The discrepancy in μ_s between theory and experiment may be a reasonable indication of the size of these omitted corrections, which are expected to be a few percent. Neglected heavy meson exchange contributions are es-

TABLE VII. 34-channel trinucleon magnetic moments.

	μ_s	μ_ν	$\mu(^3\text{He})$	$\mu(^3\text{H})$
RSC	0.4038	-2.4548	-2.0510	+2.8585
RSC+TM	0.4009	-2.4821	-2.0811	+2.8830
RSC+BR	0.3998	-2.4834	-2.0836	+2.8832
AV14	0.4058	-2.4690	-2.0632	+2.8748
AV14+TM	0.4031	-2.4961	-2.0930	+2.8993
AV14+BR	0.4020	-2.4950	-2.0930	+2.8970
(Expt.)	0.4257	-2.5532	-2.1275	+2.9789

timated to be 10% of the one-pion-exchange meson current corrections included. The fractional discrepancy between our model results and experiment is similar for both μ_ν and μ_s . In view of the nonrelativistic basis of the model Hamiltonians used and the restriction to two-pion-exchange operators in the one-body current sector, we view the agreement between theory and experiment reported here to be very reasonable.

ACKNOWLEDGMENTS

The work of J.L.F. and B.F.G. was performed under the auspices of the U.S. Department of Energy, while that of G.L.P. was supported in part by the U.S. Department of Energy. The work of E.L.T. and M.K. was supported by the National Sciences and Engineering Research Council of Canada.

-
- *Permanent address: Science University of Tokyo, Oshamanbe, Hokkaido 049-35, Japan.
- ¹C. R. Chen, G. L. Payne, J. L. Friar, and B. F. Gibson, *Phys. Rev. C* **31**, 2266 (1985).
- ²B. F. Gibson and B. H. J. McKellar, *Few-Body Syst.* (in press).
- ³J. L. Friar, B. F. Gibson, D. R. Lehman, and G. L. Payne, *Phys. Rev. C* **25**, 1616 (1982); and to be published.
- ⁴S. Ishikawa and T. Sasakawa, *Few-Body Syst.* **1**, 143 (1986).
- ⁵E. L. Tomusiak, M. Kimura, J. L. Friar, B. F. Gibson, G. L. Payne, and J. Dubach, *Phys. Rev. C* **32**, 2075 (1985).
- ⁶C. R. Chen, G. L. Payne, J. L. Friar, and B. F. Gibson, *Phys. Rev. C* **33**, 1740 (1986); *Phys. Rev. Lett.* **55**, 374 (1985).
- ⁷T. Sasakawa and S. Ishikawa, *Few-Body Syst.* **1**, 3 (1986).
- ⁸For a derivation of the various exchange current terms see, for example, M. Chemtob and M. Rho, *Nucl. Phys.* **A163**, 1 (1971) or J. L. Friar, in *New Vistas in Electro-Nuclear Physics*, Vol. 142 of *NATO Advanced Study Institute, Series B*, edited by E. L. Tomusiak, H. S. Caplan, and E. T. Dressler (Plenum, New York, 1986).
- ⁹J. L. Friar, *Phys. Rev. C* **27**, 2078 (1983).
- ¹⁰S. A. Coon and M. D. Scadron, *Phys. Rev. C* **23**, 1150 (1981).
- ¹¹D. M. Brink and G. R. Satchler, *Angular Momentum* (Clarendon, Oxford, 1968).
- ¹²P. M. Prenter, *Splines and Variational Methods* (Wiley, New York, 1975).
- ¹³J. L. Friar, B. F. Gibson, E. L. Tomusiak, and G. L. Payne, *Phys. Rev. C* **24**, 665 (1981).
- ¹⁴B. F. Gibson and L. I. Schiff, *Phys. Rev.* **138**, B26 (1965); B. F. Gibson, *Nucl. Phys.* **B2**, 501 (1967).
- ¹⁵R. Balian and E. Brezin, *Nuovo Cimento* **61B**, 403 (1969).
- ¹⁶C. R. Chen, Ph.D. dissertation, University of Iowa, 1985.
- ¹⁷See also, R. G. Sachs and J. Schwinger, *Phys. Rev.* **70**, 41 (1946).
- ¹⁸S. A. Coon, M. D. Scadron, P. C. McNamee, B. R. Barrett, D. W. F. Blatt, and B. H. J. McKellar, *Phys. Rev. C* **23**, 1790 (1981).
- ¹⁹H. T. Coelho, T. K. Das, and M. R. Robilotta, *Phys. Rev. C* **28**, 1812 (1983); M. R. Robilotta and M. P. Isidro, *Nucl. Phys.* **A414**, 394 (1984); M. R. Robilotta, M. P. Isidro, H. T. Coelho, and T. K. Das, *Phys. Rev. C* **31**, 646 (1985).
- ²⁰R. V. Reid, Jr., *Ann. Phys. (N.Y.)* **50**, 411 (1968); B. D. Day, *Phys. Rev. C* **24**, 1203 (1981) provides partial waves for $j > 2$.
- ²¹R. B. Wiringa, R. A. Smith, and T. A. Ainsworth, *Phys. Rev. C* **29**, 1207 (1984).
- ²²R. de Tourreil and D. W. L. Sprung, *Nucl. Phys.* **A201**, 193 (1984).
- ²³The error vanishes for $\Lambda \rightarrow \infty$ but increases for decreasing Λ . For $\Lambda = 5.8m_\pi$ the values of μ_{pair} in Ref. 5 should be decreased in magnitude by about 15%. Although the effect in μ_ν is only 2–3%, the error affects Tables II, IV–VI, IX and X of Ref. 5.
- ²⁴We note also that the overall sign in Eq. (19) of Ref. 5 is incorrect; it should be positive.